*Review*

# Spectroscopy of electrons excited from solids using high energy photons and electrons

L. Kövér
*Institute of Nuclear Research of the Hungarian Academy of Sciences (MTA ATOMKI)*
*18/c Bem tér, H-4026 Debrecen, Hungary*

(Received: February 14, 2006 ; Accepted: June 30, 2006)

The significance and applications of photoelectron and Auger spectroscopy excited by hard X-rays as well as spectroscopy of backscattered electrons induced from solids (2-10 keV) are discussed including necessary conditions for high energy resolution experiments, methods available for interpretation of experimental data and recent results of potential importance in chemical analysis of surface, bulk and interface layers.

## 1. Introduction

High energy resolution spectroscopy of electrons excited by hard (2-10 keV) X-rays or high energy (up to 10 keV) electrons from embedded clusters, nanostructures, buried interfaces in the case of materials of high practical importance has experienced a widespreadly growing interest recently. The rapid development of experimental technique and theoretical models in this field in the last decades makes now possible studies of fine details of electronic, chemical and physical structure of these systems, identifying and utilizing effects of condensed environment on atomic transitions.

Using high energy photons and electrons for excitation, in the respective electron spectra contributions from surface effects can be decreased and the information depth can attain several times ten nm. As a consequence, high energy resolution experiments can provide a new insight into the spatial distribution of chemical components as well as their chemical structure near buried interfaces and nanostructures. Such a way information can be obtained on the local electronic structure surrounding selected atoms (having a key importance from the point of view of certain requested functions of the given material) in the bulk region of solids or e.g. on the process of charge transfer between components of binary alloys. Combining hard X-ray induced photoelectron spectroscopy (HAXPES) with high energy resolution spectroscopy of electrons (having energies similar to those of the respective photoelectrons excited by hard X-rays) backscattered from solids, quantitative information can be gained on local chemical and electronic structures even in the case of complex materials.

In particular, in spite of the fact that the atomic subshell photoionization cross sections are strongly decreasing with increasing photon energy (*e.g.* in the case of the 1*s* core level the difference is two orders of magnitude comparing the maximum cross sections for atomic number 12 and 84 [1]), with the advantage of brighter synchrotron radiation sources (providing tunable, monochromatic and collimated hard X-ray beams), carefully designed electron optics of the electron spectrometers and multienergy detection, HAXPES has a very promising perspective.

Changing the energy of the exciting photons allows varying the information depth and makes possible to avoid the overlap of photoelectron and Auger spectra and to minimize the contribution of inelastically scattered electrons – originated from higher energy Auger transitions – to the background under the photoelectron peaks. The magnitude of surface effects in the electron spectra can be varied in a great extent as a function of the photon energy opening the way for obtaining experimental data dominated by bulk properties. Electron energy loss spectra observed using different primary electron beam energies help to separate surface and bulk scattering [2,3]. This separation is expected to be less ambiguous (*i. e.* interferences between surface and bulk excitations are expected to have a smaller role) in the case of high primary electron energies. Therefore, HAXPES can give accurate information on bulk properties of materials, important for their practical applications. Utilizing the fine tunability of the exciting photon beam, resonant studies can be performed near the core level absorption edges [4], revealing the local density of unoccupied electronic states around component atoms in the bulk. Valence band XPS spectra excited by high (5-15 keV) energy photons reflect the density of bulk electronic states weighted by the respective transition matrix elements [5]. Due to the fact, that elastic scattering is more forward peaked for high energy electrons, the linear trajectory model is a more accurate estimation for electron transport, than in the case of the conventional XPS

[5,6]. This can be advantageous in quantitative interpretation of emission angle resolved spectra containing information on the concentration depth distribution of chemical species in near surface or interface layers [6].

In the case of smooth and flat surfaces, HAXPES can provide extreme surface sensitivity as well, using grazing photon incidence (below the critical angle for total reflection) [4]. The probing depth depends very sensitively on the small (a few mrad) changes in the photon angle of incidence and the X-ray penetration depth comparable to the mean free path for inelastic electron scattering ensures this high surface sensitivity even at high energies of emitted electrons. The inelastic background is strongly suppressed in such photoelectron spectra [6].

Buried interfaces can be very effectively studied using the X-ray standing wave (XRSW) excitation by hard X-rays. XRSWs are generated by Bragg reflection from crystals or multilayers. Combining this technique with high energy resolution HAXPES, unique information can be gained on local electronic and physical structures and their spatial distribution [7].

Auger transitions between deep core atomic levels can be excited from solids using laboratory equipment as well, applying characteristic X-rays close to the photoionization threshold of the deepest level participating in the transition. The near-threshold Auger production cross section values are more than one order of magnitude higher than the respective values for electron-induced ionization and this difference approaches two orders of magnitude for elements having atomic numbers around 30 [8]. Continuous energy distribution X-rays can also be used for exciting such Auger electrons utilizing the photons available at energies higher than this threshold [8]. A recent work [9] proposes a novel X-ray source with W/Cu target for providing at least one order of magnitude higher X-ray intensities than those of existing commercial high power X-ray sources. Although standard methods for energy, resolution and efficiency calibration of electron spectrometers in the high energy range are not available yet, potentially useful methods are proposed in Ref. [10].

From accurate measurement of atomic environment induced energy shifts of deep inner-shell photoelectron lines and the corresponding Auger peaks (Auger parameter shifts), information can be derived on the local electronic structure of solids, e. g. on the charge transferred between components of binary alloys [11]. For attaining a high accuracy, analysis of deep core transitions are needed because the Auger parameter concept is valid strictly only in this case.

The purpose of the paper is to give an insight into a recently fastly developing field, the high energy and high energy resolution electron spectroscopy, using example results for illustration.

## 2. Methods of experiment and interpretation

### 2.1 Methods of experiments

For high energy XPS and XAES experiments we used our home built ESA-31 spectrometer [12] in Debrecen and the Tunable High-Energy (THE) XPS equipment of HASYLAB/DESY [13] in Hamburg, at the BW2 synchrotron beamline.

The laboratory ESA-31 instrument has a 180° hemispherical deflector energy analyzer (250 mm working radius) which provides relative $\Delta E/E$ energy resolution in the range of $10^{-3}$ – $10^{-5}$ for electrons having energies (E) from 20 eV to 10 keV. Two twin anode X-ray tubes serve as exciting photon sources (Al Kα, Ag Lα, Mo Lα, Cu Lα, Cu Kα, Cu and Mo bremsstrahlung radiation, max. 30 keV).

The THE equipment is operating at the BW2 synchrotron beamline, using a double crystal (Si(111), Si(220) and Si(311)) monochromator, ensuring $5x10^{12}$ photons on the sample in the 2.3-10 keV photon energy range. For energy analysis of photoexcited electrons a SCIENTA SES-200 hemispherical analyser is used, focusing electrons up to 5 keV (with sample bias: up to 7.5 keV). The overall energy resolution of the system is 0.2-0.5 eV. Samples can be prepared in situ using $Ar^+$ sputtering or e-beam evaporation, the structure of ordered samples can be in situ monitored during sample preparation with a built-in LEED unit.

Elastic Peak Electron Spectroscopy (EPES) and Reflection Electron Energy Loss Spectroscopy (REELS) studies are performed using the ESA-31 spectrometer equipped with two electron guns of VG LEG 62 (5 keV, 130° scattering angle) and Kimball Phys. EMG-14 (10 keV, 90° scattering angle) types.

### 2.2 Methods of interpretation

For interpretation of the experimental data calculations are performed using various models.

Modeling contributions of electron scattering to the spectra we use the QUASES-REELS method and software [14] developed by Tougaard, the Partial Intensity Analysis (PIA) method [15] elaborated by Werner and the semiclassical dielectric response model of Yubero and Tougaard [16] for describing spectral shapes and cross sections for inelastic electron scattering (XPS, XAES).

For modeling contributions from local electronic structures, cluster-approximations are applied: the Discrete Variational Xα [17] cluster molecular orbital and the Discrete Variational MultiElectron (DVME) [18] models. Initial state excitation processes are approximated by the model of Thomas [19]. Describing resonantly excited Auger peak shapes, the model of Drube developed for resonant inelastic photon-atom scattering [20] is used. Recoil effects in EPES spectra are simulated by Monte Carlo calculations [21,22].

## 3. Case studies – some recent results potentially interesting for surface/interface chemical analysis

### 3.1 High energy XPS

A key issue in the quantitative interpretation of core photoelectron and Auger spectra is the identification and separation of contributions appearing as a consequence of sudden creation of the initial core hole (intrinsic excitations) from contributions attributable to energy losses of electrons during transport within the solid (extrinsic excitations).

In the case of Ge core photoelectron and Auger lines are accompanied by intense series of plasmon satellites. Therefore the accuracy of the determination of peak intensities can depend significantly on the estimated share of intrinsic type contributions (representing integral parts of the photo- or Auger peaks).

Ge 1*s* and 2*s* photoelectron spectra were excited from polycrystalline Ge layers of 100 nm thickness using the THE XPS facility of HASYLAB [13]. The photon beam energy was 11.75 keV (Ge 1*s*) and 8 keV (Ge 2*s*), the angle of photon incidence was 45° and the angle of photoelectron emission was 0° related to the surface normal [23].

The experimental spectra were analyzed with three different models.

The simplest, Hüfner model [24] describes the normalized intensity $I_p(n)/I_0$ of the *n*th plasmon peak as [23]:

$$\frac{I_p(n)}{I_0} = \left(b^n/n!\right) + a\frac{I_p(n-1)}{I_0}$$

where *b* and *a* are fitting parameters associated with intrinsic and extrinsic excitations, respectively. Including a Poissonian statistics term for surface excitations, the modified model leads to [23]:

$$\frac{I_p(n)'}{I_0} = \left(b^n/n!\right) + a\frac{I_p(n-1)'}{I_0} + \left(c^n/n!\right)$$

with *c* standing for a fitting parameter connected with surface plasmons.

Applying the modified Hüfner model, the shape of the primary photoelectron peak was approximated by an asymmetric Doniach-Sunjic function convolved by a Gaussian, while the shapes of the plasmon satellites were derived by successive convolutions with the energy loss function derived from optical data [23].

The PIA model [15] describes the emitted spectrum $Y(E)$ as [23]:

$$Y(E) = \sum_{n_1=0}^{\infty}\sum_{n_2=0}^{\infty}\sum_{n_3=0}^{\infty} C_{n_1 n_2 n_3 \ldots} F_{n_1 n_2 n_3 \ldots}(E)$$

where the $C_{ni}$ partial intensities – *i. e.* the number of the particles participating *n* times in the *i* type of loss process, are derived by Monte Carlo simulation [25] of the elastic scattering while the corresponding partial energy loss distributions $F_{n1,n2\ldots}(E)$ are obtained convolving the primary peak by energy loss functions of the individual processes [23]. Assuming the same energy loss functions (derived from optical data) for extrinsic and intrinsic excitations and using an iterative procedure [25] the contributions of bulk and surface excitations were eliminated leaving the intrinsic spectra.

The dielectric response model [16] assumes a constant electron velocity and a stationary hole created in a semi-infinite medium. From the dielectric function (derived from optical data or from analysis of REELS spectra) the model calculates the charge density induced by electron transport or photoexcitation, and the energy loss caused by the induced field acting on the moving electron. The simulated spectrum $F(E)$ includes only the first inelastic scattering:

$$J(E) \propto \cos(\theta)\left[F(E) + \int_E^{\infty} dE' F(E')\lambda K_{SC}(E_0, E'-E, \theta)\right]$$

where $F(E)$ is the primary spectrum, $K_{sc}$ the path integrated effective cross section for inelastic scattering, $\theta$ the angle of emission; $E_0$ the primary electron energy and $\lambda$ the inelastic mean free path.

In spite of describing only the single-loss process, the dielectric response model yields a reasonable agreement with the experimental Ge 1*s* spectrum [23]. In the case of the Ge *2s* spectra all the three – i.e. the modified Hüfner, the PIA and the dielectric response models- were compared with the experimental data. For illustration, Fig. 1 shows the comparison of the simulated spectra obtained using the modified Hüfner model and the measured Ge 2*s* spectrum excited by 8000 eV photons [23]. Regarding the full spectrum, simulated by the dielectric response model the agreement is very good, similarly to the case of the modified Hüfner and the PIA models [23]. However, contributions from the second and further plasmons would modify the simulated spectrum beyond the first plasmon peak. The three models strongly differ concerning the predicted ratio of the intensities of intrinsic contributions to the total satellite peak intensity. The modified Hüfner and the PIA models yield a similar, ~ 0.2 value for this ratio, while the dielectric response model gives a ratio of ~ 0.4 [23].

It should be noted, that within the applied versions of the modified Hüfner and the PIA models, the shapes of the energy loss functions are derived from optical data and the same shape is assumed for intrinsic and extrinsic excitations. In addition, the coupling between the surface and bulk, as well as the extrinsic and intrinsic excitations are neglected. This is different for the dielectric response model, where the shape of the energy loss functions differ for electron and core hole induced losses and couplings between various excitations are accounted for in the calculations.

The results mentioned above demonstrate the significance of the issue of estimating the share of intrinsic excitations in accurate determination of peak intensities. Further

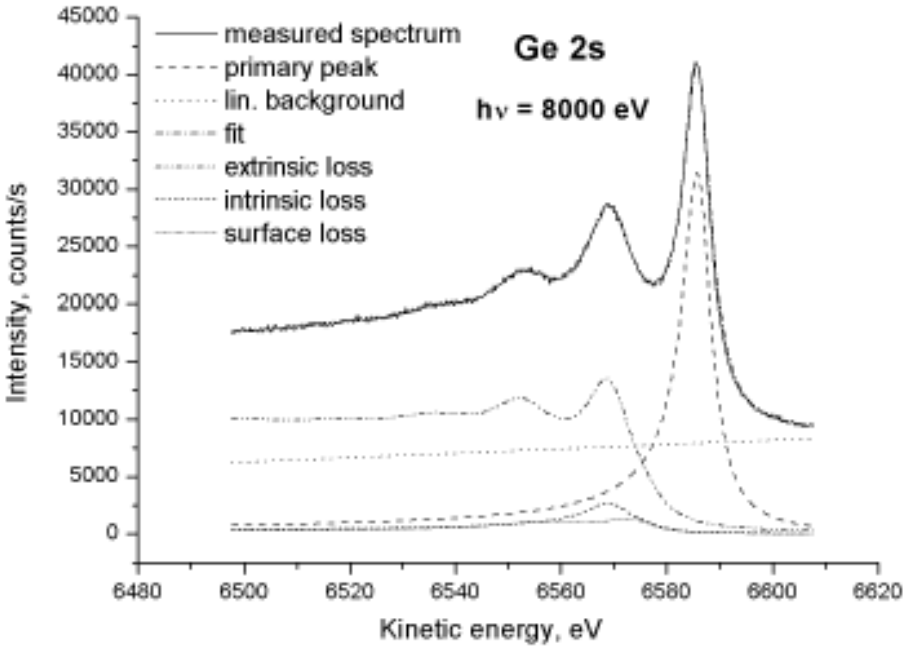


Fig. 1. The experimental Ge 2s photoelectron spectrum excited by X-rays of 8 keV energy from a Ge layer of 100 nm thickness, in comparison with the spectrum calculated using the modified Hüfner model.[23]. (Reproduced with permission from John Wiley & Sons Limited.)

studies are needed for clarifying the validity of the physical assumptions of the different approximations.

The kinetic energy dependence of intrinsic plasmon excitation was studied in the case of Si 1*s* photoelectrons excited by 3000 eV and 5500 eV photons from a Si (111) single crystal at 45° emission angle [26]. The dielectric response model predicted an appreciable increase of the normalized plasmon intensity with increasing photon energy, in agreement with the experiment, as a consequence of the decrease in screening of the core hole in the case of the faster photoelectron [26].

**3.2 High energy XAES**

Intense plasmon satellites occur in the core Auger spectra of Ge as well. Earlier works on Ge KLL Auger spectra induced by photons from thin films [27] or emitted from radioactive sources following electron capture [28] attributed these satellites to inelastic electron scattering. For estimating the role of intrinsic excitations accompanying the KLL Auger processes in Ge, the $KL_{23}L_{23}$ spectra, induced from polycrystalline Ge films of 100 nm thickness were measured with an energy resolution of 2.6 eV (at 8.5 keV electron energy) using bremsstrahlung radiation and the ESA-31 spectrometer [29]. Inelastic background correction was performed using the method of Tougaard [14] and applying the cross section for inelastic electron scattering [30] derived from REELS spectra obtained from the same sample with primary electron energy of 8 keV. The REELS spectra were dominated by an intense series of plasmon peaks and the energy separation between the first plasmon peak and the elastic peak ( 16 eV) was found to agree well with the satellite – main $^1D_2$ peak energy separation (15.7 eV) in the photoinduced $KL_{23}L_{23}$ Auger spectra [29]. On the basis of atomic calculations and the "excited atom model" for screening [31] the assignment of the Auger satellite as due to initial state shakeup excitation, can be ruled out. This confirms that the origin of the satellite is attributable to plasmon creation. Following correction for inelastic background, a significant portion of the satellite intensity remained [29] indicating the presence of contributions from intrinsic plasmon excitations. For modeling these excitations, the dielectric response model [16] was used, calculating the effective cross sections for core-hole (assuming two holes corresponding to the two final state core holes of the Auger process) potential induced intrinsic losses as well as for electron transport induced extrinsic losses. Convolution of the path integrated intrinsic, extrinsic and total effective cross sections by a model Lorentzian representing the primary peak leads to the respective simulated spectra. In Fig. 2 the comparison between the measured Ge $KL_{23}L_{23}$ spectrum (corrected removing a smooth integral background for making the comparison easier) and the simulated spectrum obtained using the dielectric response model [29] is shown.

The agreement is quite reasonable, in spite of that the model describes only a single loss and the $^1S_0$ diagram Auger peak is not considered in the simulated spectrum. For deriving the share of intrinsic excitations in plasmon creation, the probability that the energy loss of the electrons

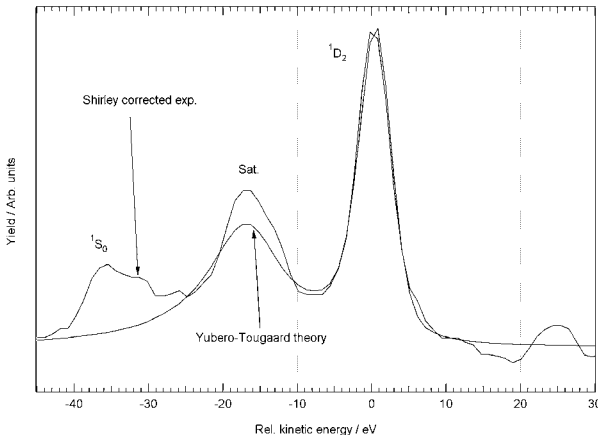


Fig. 2. The experimental Ge $KL_{23}L_{23}$ Auger spectrum excited by bremsstrahlung from a Ge layer of 100 nm thickness, in comparison with the spectrum calculated using the dielectric response model of Yubero and Tougaard [29]. (Reproduced with permission from Elsevier.)

appearing in the plasmon satellite peak was caused by intrinsic or extrinsic excitations was determined by fitting the main $^1D_2$ diagram Auger peak and the plasmon peak by asymmetric Lorentzians in the measured and in the respective (hole, electron or total) simulated model spectra. The ratio of the intensity of the respective plasmon peak to the intensity of the main peak was defined as the intrinsic, extrinsic or total plasmon excitation probabilities. To obtain the theoretical value for the share of intrinsic plasmon excitations, first the effect of electron transport, *i. e.* the path length integrated effective inelastic cross section describing electron induced energy losses, was used and the corresponding simulated spectrum reflecting extrinsic plasmon losses was calculated. Then, the total plasmon peak was simulated by taking into the account in addition the effect of the remaining core holes in the effective inelastic cross section. Considering that the total plasmon excitation probability is the sum of the intrinsic and extrinsic plasmon excitation probabilities, the share of intrinsic excitation was derived from the evaluated plasmon intensities [29]. It should be noted that in this approximation the coupling between extrinsic and intrinsic excitations was neglected when estimating the intrinsic share. From these the theoretical intrinsic share was found to be 40 %. This result is consistent with the estimation of the dielectric response model in the case of the Ge *2s* spectrum [24]. The experimental intrinsic share was obtained from the evaluated plasmon intensity, fitting the integral background corrected Auger spectrum (the total plasmon intensity containing contributions from both extrinsic and intrinsic excitations) and from the plasmon intensity fitting the plasmon peak remained after inelastic background correction using REELS cross section for inelastic scattering (the plasmon intensity containing contributions only from intrinsic excitations) [29]. The ratio of these plasmon intensities, the experimental intrinsic share was found to be 31 % [29], in a good agreement (within the experimental error) with the estimation of the dielectric response model.

While the dielectric response model describes the first intrinsic plasmon excitation, the analysis of the complete Ge $KL_{23}L_{23}$ spectrum indicates [32] that accounting for the second intrinsic plasmon and assuming a Poissonian distribution for intrinsic plasmon intensities is necessary for achieving a consistency with atomic calculations and with the Ge KLL spectra emitted from very thin radioactive samples [28]. In Fig. 3. the decomposition of a photoexcited Ge $KL_{23}L_{23}$ spectrum is shown, after inelastic background correction using REELS cross section for inelastic electron scattering

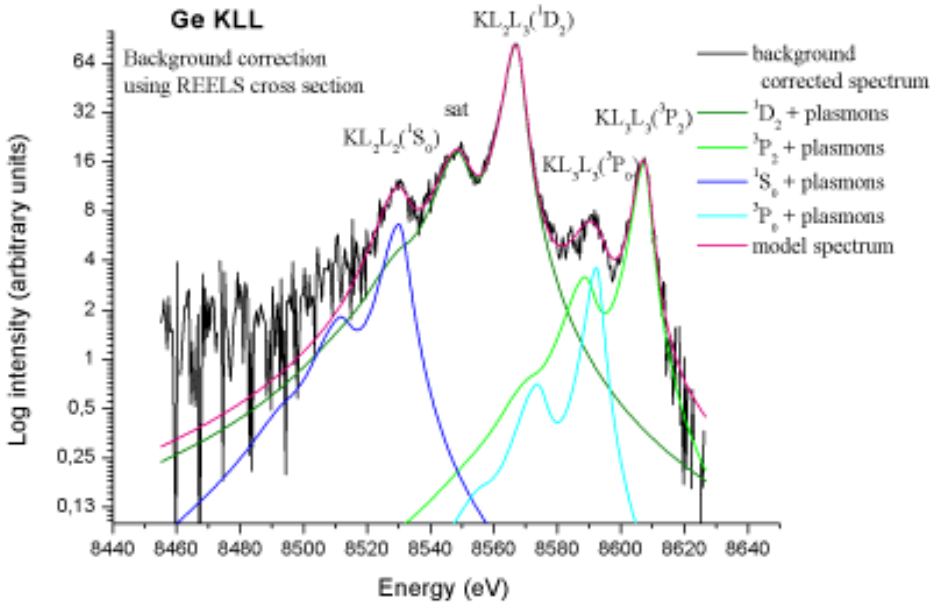


Fig. 3. Decompositon of the Ge $KL_{23}L_{23}$ Auger spectrum (shown in Fig. 2), accounting for multiple plasmon excitations.

[33].

Although the effect of solid environment on photoexcited deep core Auger spectra is very significant as demonstrated above, the multiplet splitting of the Auger transitions show only a negligible solid state effect. In the case of *3d* transition metals the energy splittings of the KLL Auger multiplets were calculated for free atoms and metal clusters using a many electron method based on configuration interaction and fully relativistic molecular orbital theory [34]. The obtained multiplet splittings between the $^3P_2$ ($KL_3L_3$) and $^1S_0$ ($KL_2L_2$) terms are smaller for metal clusters than for free atoms by about 0.2 eV only and the calculated multiplet energies are close to the recent experimental values [34].

**3.3 High energy REELS**

Experimental high energy resolution REELS spectra induced by energetic electrons are important from the point of view of correct interpretation of high energy (2-15 keV) photoelectron or Auger electron spectra excited by hard X-rays. In Fig. 4 the REELS spectrum obtained from a polycrystalline Ge film of 100 nm thickness using a primary electron beam of 8 keV energy (close to the kinetic energy of the main $^1D_2$ line of the Ge $KL_{23}L_{23}$ Auger spectra) [29] can be seen. The angle of the incident primary electron beam was 50°, while the angle of emission of the detected scattered electron beam was 0° relative to the surface normal of the sample.

The spectrum is dominated by the intense series of plasmon loss peaks, attributable to multiple plasmon excitations.

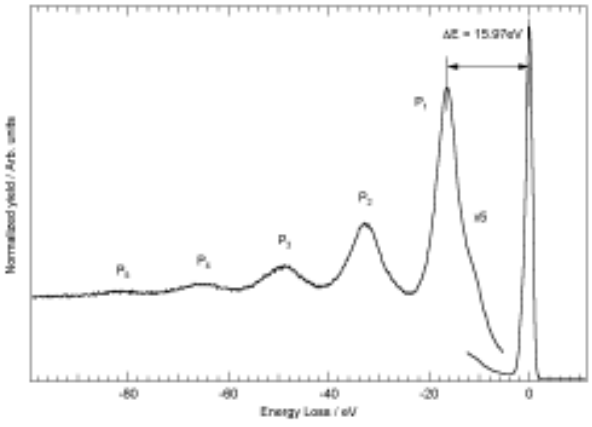


Fig.4. REELS spectrum of a Ge film of 100 nm thickness induced using primary electrons of 8 keV energy [29]. (Reproduced with permission from Elsevier.)

At the higher kinetic energy side of the first plasmon peak, a shoulder appears as a consequence of the presence of surface plasmon excitations indicating that even in the case of such a high energy electrons, the role of surface excitations induced by the primary or scattered electrons when crossing the surface is non-negligible. From analysis of the experimental REELS spectra cross sections for inelastic scattering of electrons losing energy through bulk and surface excitations, can be derived. Employing the recursion formula of Tougaard and Chorkendorff [35] based on the *P1* approximation to the Boltzmann equation, the effects of multiple inelastic scattering can be removed from the REELS spectra and the cross section for inelastic electron scattering can be obtained. At high primary electron energy – where surface effects have smaller contributions - this procedure yields inelastic cross sections comparable to those calculated using the Lindhard-Ritchie theory [30]. A recent method of Werner [3] is based on the simultaneous deconvolution of two experimental REELS spectra measured in different experimental conditions (primary beam energy or geometrical configurations), using an algorithm for reversion of a bivariate power series in the Fourier space to yield an unique solution providing the normalized differential mean free path for inelastic electron scattering (DIIMFP) and the normalized differential surface excitation probability (DSEP). DIIMFP and DSEP functions derived from simultaneous deconvolution of REELS spectra measured using 1 and 3 keV primary electron beams in the case of Fe, Pd and Pt surfaces [3] show a quite reasonable agreement with the dielectric theory of Tung [36]. Analyzing two REELS spectra taken at different primary electron energies and varying the parameters which describe a dielectric function until a good agreement is reached between the experimentally derived and theoretical inelastic cross sections, the accurate dielectric function of the material can be obtained [2,37]. Then this dielectric function can serve as an input to the dielectric response model [16] for simulating XPS or Auger lineshapes [2].

Surface excitation parameter (SEP) is an important parameter for describing surface excitations. SEP is the average number of surface excitations occurring at a single surface crossing by a primary or scattered electron. The probability of the multiple surface excitations is assumed to be described by a Poissonian distribution. As a consequence, the SEP determines the probability of a given number of surface excitations. Applying a new method based on the elimination of multiple bulk inelastic electron scattering from the REELS spectra by the help of a deconvolution procedure using partial intensities and partial energy losses, the differential surface excitation probability can be retrieved [38]. DSEPs and SEPs were determined from experimental REELS spectra using this new method in the case of Si, Ni, Ge and Ag surfaces and 0.2-5 keV primary electron energy [39]. The angle of the incident electron beam was 50°, while the angle of the detected scattered electrons was 0° relative to the surface normal of the sample. To eliminate the contribution from multiple scattering in the bulk, energy loss fuctions derived from optical data and partial intensities obtained

from Monte Carlo simulations were used [39] as input parameters. The extracted DSEPs clearly show the effect of the depolarization of the bulk near the surface (begrenzung). For Si and Ge the DSEP curves agree well with Tung's theory [36], except the vicinity of the elastic peak [39]. In the case of Ni and Ag, although the overall agreement between experiment and theory is reasonable, significant deviations occur, possibly due to the deficiencies in the optical data used. The SEPs derived from the DSEP curves show larger scatter when comparing to data from earlier measurements and from theory. Determining SEPs, a material parameter is derived from the measurements for describing the energy and emission angle dependence of SEPs.

**3.4 High energy EPES, IMFPs for high energy electrons**

With the increasing significance and applications of the spectroscopy of electrons induced by hard X-rays or energetic photons, the need for accurate and reliable parameters used in quantitative interpretation of the observed spectra, becomes stronger. Such an important quantity is the inelastic mean free path (IMFP) of the electrons in the solid. The main reason for the lack of available experimental IMFPs for high electron energies is that the experimental conditions requested are far beyond those of conventional in surface analytical applications of electron spectrometers. The intensity of the elastic peak in the spectra of electrons backscattered from the sample surface contains information on the IMFP. To determine IMFPs experimentally, the EPES method [40] is used widely. Within this method, the measured elastic-backscattering yields of a given and a reference sample (with known IMFP) is determined and for obtaining the unknown IMFP, Monte Carlo simulations of electron scattering are performed as a function of the IMFP (free parameter). From the measured ratio of the elastic peak intensities of the analyzed and the reference sample, the IMFP dependence of the simulated elastic backscattering probabilities and from the IMFP of the reference sample, the IMFP for the sample material can be derived. As a consequence, the accuracy of the EPES method depends on the accuracy and reliability of the data of the reference data used.

High energy resolution EPES measurements were performed using polycrystalline thin film Ge and Ag (reference) samples with the purpose of determining the IMFPs in Ge in the electron energy range 2-10 keV [41]. For primary electron beam energies above 5 keV, an accelerating positive sample bias was applied. The energy resolution of the electron spectrometer was between 0.09 and 0.45 eV. Calculating elastic-backscattering probabilities, the Monte Carlo simulation software [42] developed by Jablonski was used with differential cross sections for elastic scattering taken from the NIST database [43]. Calculating the backscattering probabilities as functions of the IMFP of the sample and of the reference material, respectively, and using the ratio determined from the measured elastic yields of the analyzed sample, the IMFPs of the sample can be plotted against the IMFPs of the reference material. Selecting IMFP values (as a function of the electron energy) published earlier for the reference material, the IMFPs in the analyzed sample can be read out easily from the plots.

The advantage of this presentation of data (the "lambda-lambda" curve) [41] is that choosing a new (e.g. more accurate) reference IMFP value, by the help of this curve the new IMFP value for the analyzed material can be seen immediately. In this particular case of Ge, Ag was selected as reference material and the reference IMFPs [44] calculated from optical data using Penn's algorithm were used. The so determined EPES IMFPs for Ge (as a function of electron energy 2-10 keV) are shown in Fig. 5., in comparison with values obtained using different formulae [41]. It should be noted that the largest uncertainty in the determined values can be attributed to the uncertainty of the elastic-scattering probabilities derived from the Monte Carlo simulations. Both

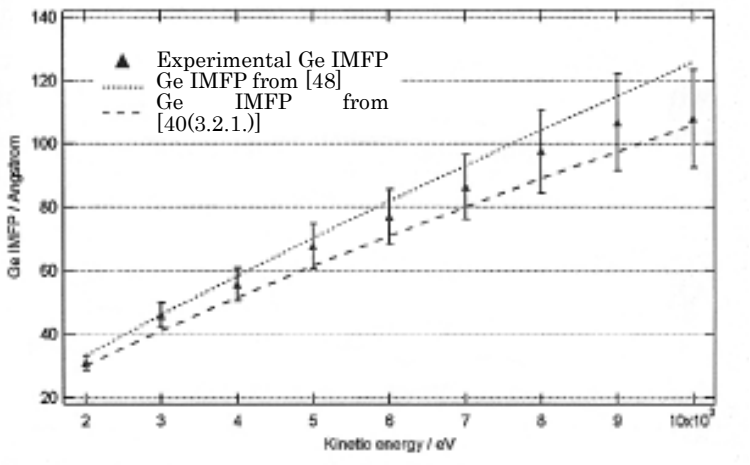


Fig. 5. Ge IMFPs determined using the EPES method, in comparison with different predictions [41]. (Reproduced with permission from Elsevier.)

earlier estimations are consistent with the EPES IMFP data although at higher energies the EPES data are closer to those predicted by Powell and Jablonski [40].

IMFPs can be determined from shape analysis of high energy electron spectra as well, because the inelastic background strongly depends on the IMFP. Using the QUASES shape analysis (based on the "universal" cross section for inelastic electron scattering) [14] of hard X-ray induced K-Auger spectra of Cu, Ni and Co thin (5-40 nm thick) films as well as of Fe K-conversion spectra (induced by nuclear decay of $^{57}$Co source) attenuated by Au overlayers of various (2.7-20.8 nm) thicknesses, the IMFP values in Ni, Cu, Co and Au for electron energies 6-7.5 keV were determined [45]. The peak shape analysis resulted in consistent IMFP values for different film thicknesses and in the case of Co for different energy electrons (from different transitions) [45]. Comparing the results to respective IMFP values published earlier, a quite reasonable agreement was found [45], confirming the applicability of the peak shape analysis in the case of high energy electron spectra excited from thin films of known thickness for deriving IMFPs.

### 3.5 Spectroscopy based on atomic recoil effects in high energy EPES

Using the classical approach describing single elastic electron scattering on free atoms assumed to have zero kinetic energy, the energy $E_{rec}$ transferred to the recoiled scattering atom is [46]:

$$E_{rec} = (4m/M)E_0 \sin^2(\theta/2)$$

where $m$ and $M$ denote the mass of the electron and the scattering atom, respectively, $E_0$ the primary energy of the electron and $\theta$ is the scattering angle. Assuming that the scattering atoms (like free atoms) have a Maxwell-Boltzmann thermal energy distribution with an average kinetic energy $\varepsilon$, an isotropic distribution for the direction of their velocity, the resulting Doppler broadening of the elastic peak will have a Gaussian distribution with a full width at half maximum $\Delta E_r$ [47]:

$$\Delta E_r = 4(2/3\, E_{rec}\, \varepsilon \ln 2)^{1/2}$$

From the equations above it can be seen, that $E_{rec}$ is increasing with primary electron energy and decreasing with increasing mass of scattering atoms while $\Delta E_r$ depends on the square root of the ratio of the primary energy and the mass of scattering atoms. Therefore clearly observable recoil energy shifts $\Delta E_r$ are expected to occur at high electron energies and low $M$. On the other hand, in this case the Doppler broadening is higher.

This phenomenon gives a unique possibility to detect hydrogen atoms by high energy resolution EPES [22]. Fig. 6 shows an EPES spectrum excited by primary electrons of 2 keV energy from polyethylene [22].

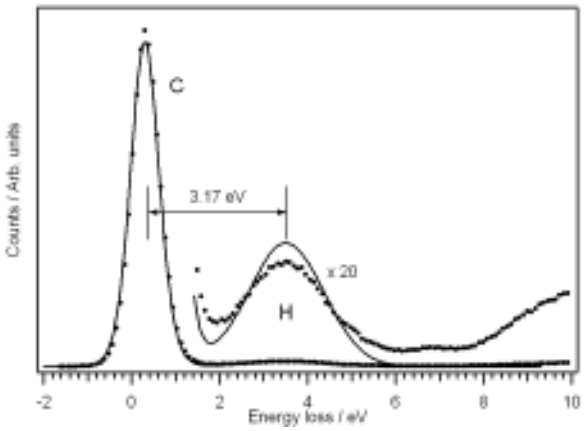


Fig. 6. REELS spectrum of polyethylene obtained using primary electrons of 2 keV energy (dots) compared to Monte Carlo simulation (solid line) [22]. (Reproduced with permission from John Wiley & Sons Limited.)

The elastic peak is split to a high intensity peak attributable to electrons scattered elastically on C atoms and a very low intensity, but clearly resolved peak due to elastic scattering on H atoms. The good agreement between the experimental EPES spectrum and the result of Monte Carlo simulation of electron scattering in polyethylene derived on the basis of the classical approach [22] shows the potential applicability of this spectroscopy for quantitative surface analysis. Experimental results on recoil shifts using high energy primary electrons [46, 47] confirm the validity of the classical approach in the case of selected solids.

In a recent work of Fujikawa et al. [49] quasi-elastic scattering of high energy electrons is studied with quantum scattering theory including atomic recoil effects. For free atoms the theory yields the classical results and this is also the case for solids in the high temperature region and when the Debye approximation for phonon modes is valid [49]. Effects of atomic recoil during emission of photoelectrons excited by hard X-rays from solids were also described with this theory, providing simple formulas within the Debye approximation for recoil shifts and Doppler broadenings [49]. The calculations show that the Franck-Condon effects play only minor role in elastic peak shifts and broadenings, and that for light elements the recoil shifts are comparable with typical chemical shifts in conventional XPS.

### 4. Summary

Spectroscopy of electrons having energy of 2-10 keV and excited from solids using high energy photons and electrons is – as a consequence of recent developments concerning new generations of synchrotron X-ray sources, high energy resolution electron spectrometers and theoretical models for interpretation of electron spectra at different lev-

els – a very promising tool for accurate quantitative chemical analysis of surface, interface and bulk regions of solids, with the option of identifying and determining embedded local physical and electronic structures on a cluster, molecule or atomic scale.

**Acknowledgements**

This work was supported by the European Community-Research Infrastructure Action under the FP6 "Structuring the European Research Area" Programme (through the Integrated Infrastructure Initiative) Integrating Activity on Synchrotron and Free Electron Laser Science, as well as by the grant OTKA T038016.

**References**

[ 1 ] J. H. Scofield, *Lawrence Livermore Laboratory Report* UCRL-51326(1973).
[ 2 ] S. Tougaard, F. Yubero, *Surf. Interface Anal.* **36,** 824 (2004).
[ 3 ] W. S. M. Werner, *Surf. Sci.* **588,** 26 (2005).
[ 4 ] W. Drube, *Nucl. Instrum. Meth. Phys. Res.* A **54,** 87 (2005).
[ 5 ] W. S. M. Werner, L. Kövér, J. Tóth, D. Varga, J. *Electron Spectrosc. Relat. Phenom.* **122,** 103 (2002).
[ 6 ] C. S. Fadley, *Nucl. Instrum. Meth. Phys. Res.* A **54,** 24 (2005).
[ 7 ] J. C. Woicik, E. J. Nelson, I. Kronik, M. Jain, J. R. Chelikowsky, D. Heskett, L. E. Berman, G. S. Herman, Phys. Rev. Lett. **89,** 077401 (2002).
[ 8 ] L. Kövér, A. Némethy, I. Cserny, D. Varga, *Surf. Interface Anal.* **20,** 659 (1993).
[ 9 ] K. Araki, A. Yoshioka, R. Shimizu, T. Nagatomi, S. Takahashi, Y. Nihei, *Surf. Interface Anal.* **33,** 376 (2002).
[10] L. Kövér, *Surf. Interface Anal.* **33,** 269 (2002).
[11] L. Kövér, in : *Hartree-Fock –Slater Method for Materials Science*, Eds.: H. Adachi, T. Mukoyama, J. Kawai, *Springer Series in Materials Science, Springer Verlag*, 2006, p.209.
[12] L. Kövér, D. Varga, I. Cserny, J. Tóth, K. Tõkési, *Surf. Interface Anal.* **19,** 9 (1992).
[13] W. Drube, T. M. Grehk, R. Treusch, G. Materlik, *J. Electron Spectrosc. Relat. Phenom.* **88-89,** 683 (1998).
[14] S. Tougaard, QUASES: *Software package for Quantitative XPS/AES of Surface Nanostructures by Peak Shape Analysis*, Ver. 5.0 (2002) www.quases.com
[15] W. S. M. Werner, *Surf. Interface Anal.* **23,** 737 (1995).
[16] A. C. Simonsen, F. Yubero, S. Tougaard, *Phys. Rev.* B **56,** 1612 (1997).
[17] H. Adachi, M. Tsukada, C. Satoko, *J. Phys. Soc. Jpn* **45,** 875 (1978).
[18] K. Ogasawara, T. Iwata, Y. Koyama, T. Ishii, I. Tanaka, H. Adachi, *Phys. Rev.* B **64,** 115413 (2001).
[19] T. D. Thomas, *Phys. Rev. Lett.* **52,** 417 (1984).
[20] W. Drube, R. Treusch, G. Materlik, *Phys. Rev. Lett.* **74,** 42 (1995).
[21] D. Varga, K. Tõkési, Z. Berényi, J. Tóth, L. Kövér, G. Gergely, A. Sulyok, *Surf. Interface Anal.* **33,** 1019 (2001).
[22] D. Varga, K. Tõkési, Z. Berényi, J. Tóth, L. Kövér, *Surf. Interface Anal.*, **38**, 544 (2006).
[23] L. Kövér, M. Novák, S. Egri, I. Cserny, Z. Berényi, J. Tóth, D. Varga, W. Drube, F. Yubero, S. Tougaard, W.S.M. Werner, *Surf, Interface Anal.*, **38**, 569 (2006).
[24] S. Hüfner, *Photoelectron Spectroscopy* (3rd edn.), Springer, Berlin, (2003) p. 112.
[25] W.S.M. Werner, *Surf. Interface Anal.* **33,** 141 (2001).
[26] F. Yubero, L. Kövér, W. Drube, Th. Eickhoff, S. Tougaard, *Surf. Sci.* **592,** 1 (2005).
[27] E. Sokolowski, C. Nordling, *Arkiv för Fysik* **14,** 557 (1958).
[28] A. Kovalík, E. A. Yakushev, D. V. Filosofov, V. M. Gorozhankin, Ts. Vylov, *J. Electron Spectrosc. Relat. Phenom.* **123,** 65 (2002).
[29] Z. Berényi, L. Kövér, S. Tougaard, F. Yubero, J. Tóth, I. Cserny. D. Varga, *J. Electron Spectrosc. Relat. Phenom.* **135,** 177 (2004).
[30] S. Tougaard, J. Kraaer, *Phys. Rev.* B **43,** 1651 (1991).
[31] I. Cserny, L. Kövér, H. Nakamatsu, T. Mukoyama, *Surf. Interface Anal.* **30,** 199 (2000).
[32] L. Kövér, S. Egri, Z. Berényi, J. Tóth, I. Cserny, D. Varga, to be published.
[33] L. Kövér, S. Egri, I. Cserny, Z. Berényi, J. Tóth, J. Végh, D. Varga, *J. Surf. Anal.* **12,** 146 (2005).
[34] T. Ishii, L. Kövér, Z. Berényi, I. Cserny, H. Ikeno, H. Adachi, W. Drube, *J. Electron Spectrosc. Relat. Phenom.* **137-140,** 451 (2004).
[35] S. Tougaard, I. Chorkendorff, *Phys. Rev.* B **35,** 6570 (1987).
[36] C. J. Tung, Y. F. Chen, C. M. Kwei, T. L. Chou, *Phys. Rev.* B **49,** 16684 (1994).
[37] F. Yubero, S. Tougaard, E. Elizalde, J. M. Sanz, *Surf. Interface Anal.* **20,** 719 (1993).
[38] W. S. M. Werner, *Surf. Sci.* **526,** L159 (2003).
[39] W. S. M. Werner, L. Kövér, S. Egri, J. Tóth, D. Varga, *Surf. Sci.* **585,** 85 (2005).
[40] C. J. Powell, A. Jablonski, *J. Phys. Chem. Ref. Data* **28,** 19 (1999).
[41] Z. Berényi, B. Aszalós-Kiss, J. Tóth, D. Varga, L. Kövér, K. Tõkési, I. Cserny, S. Tanuma, *Surf. Sci.* **566-568,** 1174 (2004).
[42] A. Jablonski, P. Jiricek, *Surf. Sci.* **42,** 412 (1998); A. Jablonski, *Surf. Interface Anal.* **37**, 1035 (2005).
[43] NIST Elastic-Electron-Scattering Cross Section Database, Version 2.0. Standard Reference Data Program, Database 64, April 2000. National Institute of Standards and Technology, Gaithersburg, MD, USA. The more recent version of this database (with more reliable data) is Version 3.0 (2003).
[44] S. Tanuma, C. J. Powell, D. R. Penn, in press.

[45] L. Kövér, S. Tougaard, J. Tóth, D. Varga, A. Kovalík, M. Ryšavy, *J. Surf. Anal.* **9,** 281 (2002).
[46] H. Boersch, R. Wolter, H. Schoenebeck, *Z. Physik* **199,** 124 (1967).
[47] D. Varga, K. Tõkési, Z. Berényi, J. Tóth, L. Kövér, G. Gergely, A. Sulyok, *Surf. Interface Anal.* **31,** 1019 (2001).
[48] S. Tanuma, C. J. Powell, D. R. Penn, *Surf. Interface Anal.* **17,** 911 (1991).
[49] T. Fujikawa, R. Suzuki, L. Kövér, *J. Electron Spectrosc. Relat. Phenom.* **151,** 170 (2005).